Unusual Temperature Dependence of Proton Transfer. 2. Excited-State Proton Transfer from Photoacids to Water

Boiko Cohen, Pavel Leiderman, and Dan Huppert*

Raymond and Beverly Sackler Faculty of Exact Sciences, School of Chemistry, Tel Aviv University, Tel Aviv 69978, Israel

Received: June 2, 2002; In Final Form: September 9, 2002

We measured the proton-transfer rate constant from a strong and a weak photoacid to water as a function of temperature. We found that the proton-transfer rate constant for the strong photoacid at high temperatures, $T > 300$ K, is almost temperature-independent, whereas at low temperatures, $T < 300$ K, the rate constant exhibits a strong temperature dependence. For the weak photoacid, the rate constant also exhibits a relatively large activation energy in the high-temperature region. Previously, we found that the temperature dependence of the proton-transfer rate constant to alcohols is explained as a continuous transition from nonadiabatic to solvent-controlled limits. The model we used to calculate the proton-transfer rate constant is based on the diffusive propagation of the solvent configuration along a generalized solvent coordinate from the reactant potential surface toward the crossing point with the product potential surface. The proton transfer occurs at the crossing point, and the rate is calculated by a sink term placed at the crossing point. The sink term includes the solvent velocity and the Landau−Zener transmission coefficient. Both the diffusion constant and the Landau−Zener transmission coefficient depend on the dielectric relaxation of the solvent. The calculations are compared with the experimental data and an interpolation expression that bridges the nonadiabatic limit and the solvent-controlled limit.

Introduction

In their excited states, photoacids and photobases are stronger acids or bases, respectively. Excitation of these compounds in a solution of protic solvents enables the study of the dynamics of the proton-transfer reactions of acids and bases in solution.[1−6]

In recent papers,[7−10] we described our experimental results of an unusual temperature dependence of excited-state proton transfer from a super photoacid (5,8 dicyano-2-naphthol, DCN2) to several monols, diols, and a glycerol. At relatively high temperatures, the rate of proton transfer is almost temperature-independent, whereas at relatively low temperatures, the rate exhibits great temperature dependence, and the rate-constant value is similar to the inverse of the dielectric relaxation time. We proposed a simple stepwise model to describe and calculate the temperature dependence of the proton transfer to the solvent. The model accounts for the large differences in the temperature dependence and the proton transfer rate at high and low temperatures.

The temperature dependence of the rate constant for proton transfer to the protic solvent is explained as a continuous transition from nonadiabatic (high temperature) to solvent-controlled (low temperature) proton transfer. This phenomenon can be described by the Landau−Zener curve-crossing equation[11,12] for the proton-transfer rate constant.

The theoretical analysis for the solution-phase proton-transfer reaction was undertaken by Dogonadze, Kuznetzov, Ulstrup, and co-workers[13−17] and then extended by Borgis and Hynes,[18−20] Cukier,[21,22] and Voth.[23,24] These theories suggest that, when a potential energy barrier is present in the proton-reaction coordinate, the reaction pathway involves tunneling through the barrier, as opposed to passage over the barrier. The proton transfer can be described as quantum tunneling between two wells formed by two interacting electronic states. The transfer of the proton from one well to the other is associated with a change in the electronic state of the system. The crossover between the electronic states can occur only when the proton tunnels through the barrier.

Conventional Landau−Zener (LZ) theory[11,12] provides an accurate description of the process in the absence of interaction with the environment. It is applicable if the motion in the vicinity of the crossing point is nearly uniform (ballistic).[25,26] The interaction of the particle with the environment causes complications. The curve-crossing problem in the presence of dissipation has been studied extensively.[27−35] Expressions for the transition rate of various physical limits has been derived. When the coupling, V, between the diabatic terms is the smallest parameter of the system, the dynamics in the crossing region in this *nonadiabatic* limit is fast, the tunneling rate is the rate-limiting step, and the reaction rate is given by the Fermi Golden Rule expression. When the coupling between the diabatic states is larger than k_BT, the adiabatic representation of the coupled potential energy surfaces is adequate, the upper adiabatic potential surface plays a negligible role, and the rate expression is given by the standard transition-state theory (TST) equation. Another physical limit is realized when $V \leq k_BT$ and the interaction with the environment is strong enough. In this solvent-controlled limit, the rate is inversely proportional to the solvent relaxation time (friction) and is independent of the coupling V.

In this study, we measure the temperature dependence of the proton transfer from two photoacids to water. We chose two photoacids that differ in their acidity in the excited state, pK*, and their proton-transfer rate constants. The temperature de-

* Corresponding author. E-mail: huppert@tulip.tau.ac.il. Fax/phone: 972-3-640-7012.

10.1021/jp026223o CCC: $22.00
Published on Web 10/23/2002

SCHEME 1

$$\mathrm{ROH^*} \underset{k_r}{\overset{k_d}{\rightleftharpoons}} [\mathrm{RO^-}^* \ldots \mathrm{H^+}]_{(r=a)} \overset{\mathrm{DSE}}{\rightleftharpoons} \mathrm{RO^-}^* + \mathrm{H^+}$$

pendence of the stronger photoacid (2-naphthol-6,8-disulfonate, 2N68DS, pK^* = 0.4) in water has similar behavior to that which we found for DCN2 for several alcohols. At relatively high temperatures, the rate of proton transfer is almost temperature-independent, whereas at relatively low temperatures, the rate exhibits great temperature dependence. The temperature dependence of the proton-transfer rate constant of the weaker photoacid, 2-naphthol (pK^* = 2.7), exhibits different behavior. The activation energy of the proton-transfer process is about 12 kJ/mol at high temperatures. At low temperatures, $T < 300$ K, the activation energy increases and reaches $\Delta G^{\ddagger} = 20$ kJ/mol at 250 K.

Experimental Section

Time-resolved fluorescence was measured using the time-correlated single-photon counting (TCSPC) technique. As an excitation source, we used a CW mode-locked Nd:YAG-pumped dye laser (Coherent Nd:YAG Antares and a 702 dye laser) providing a high repetition rate (>1 MHz) of short pulses (2 ps at full width at half-maximum, fwhm). The (TCSPC) detection system is based on a Hamamatsu 3809U photomultiplier, Tennelec 864 TAC, Tennelec 454 discriminator, and personal computer-based multichannel analyzer (nucleus PCA-II). The overall instrumental response was about 50 ps (fwhm). Measurements were taken at 10-nm spectral widths. Steady-state fluorescence spectra were taken using an SLM AMINCO-Bowman-2 spectrofluoremeter.

2-Naphthol-6,8-disulfonate (2N68DS) was purchased from Eastman Kodak, and 2-naphthol (2N), from Riedel-De Haen (Hanover). The sample concentrations were between 2×10^{-4} and 2×10^{-5} M. Deionized water had a resistance >10 MΩ. The solution's pH was about 6.

The photoacids' fluorescence spectrum consists of two structureless broad bands (~40 nm fwhm). The emission-band maximum of the acidic form (ROH*) emits at higher energies than the emission-band maximum of the alkaline form (RO^-*). At the ROH* emission-band maximum, the overlap of the two luminescence bands is rather small, and the contribution of the RO^-* band to the total intensity is about 0.5%. In addition, we find that a fluorescent impurity in the compounds increases the fluorescence intensity at long times to the level of 0.1−0.5% of the peak intensity. Therefore, in the time-resolved analysis, we add to the calculated signal an additional exponential decay of about 10 ns with an amplitude in the range of 0.1−0.5% to compensate for the impurity fluorescence.

The temperature of the irradiated sample was controlled by placing the sample in an oven or a liquid N_2 cryostat with thermal stability of approximately ±1 K.

Modeling

Proton Dissociation and Geminate Recombination in the Liquid Phase. Experimental and theoretical studies of ESPT processes in solution have led to the development of a two-step model[36,37] (Scheme 1).

The first step is described by back-reaction boundary conditions with intrinsic rate constants k_d and k_r. This is followed by a diffusional second step in which the hydrated proton is removed from the parent molecule. This latter step is described by the Debye−Smoluchowski equation (DSE). In the continuous-diffusion approach, one describes the photoacid dissociation reaction by the spherically symmetric diffusion equation (DSE)[38] in three dimensions.[36,37] The boundary conditions at $r = a$ are those of the back reaction (Scheme 1). k_d and k_r are the "intrinsic" dissociation and recombination rate constants, respectively, at the contact-sphere radius a. Quantitative agreement was obtained between theory and experiment,[36,37] and as a result, it was possible to make a more detailed study of the ESPT process itself as well as of the dynamic and static properties of the solvent.

An important parameter in our model is the mutual diffusion coefficient $D = D_{H^+} + D_{RO^-}$. The temperature dependence of the proton diffusion constant, D_{H^+}, in water was deduced from the proton conductance measurements as a function of T.[39,40] The anion diffusion constant, D_{RO^-}, as a function of T was estimated from the solvent viscosity data.[41,42] The temperature dependence of the dielectric constant and the dielectric relaxation of water data were taken from refs 39, 43, 44, and 45. Using Scheme 1 and the numerical solution of the DSE, we fitted the experimental data and extracted both the intrinsic proton dissociation and recombination (k_d and k_r) rate constants. Typical chi-squares of the fit range from 1.2 to 2. We determined the proton-transfer rate constant, k_d, from the fit to the initial fast decay of the ROH* fluorescence. The initial fast component of the fluorescence decay is mainly determined by the deprotonation process and is nearly insensitive to the geminate recombination process. The long-time behavior (the fluorescence tail) seen in the ROH* time-resolved emission is a consequence of the repopulation of the ROH* species by the reversible recombination of RO^-* with the geminate proton. The reprotonation is an adiabatic process, and therefore the excited ROH* can undergo a second cycle of deprotonation. The overall effect is a nonexponential fluorescence tail.

The comparison of the numerical solution with the experimental results involves several parameters. Some are adjustable parameters, such as k_d and k_r, and others, such the contact radius a, have acceptable literature values.[36,37] We are facing a multiparameter problem in adjusting a solution of a partial differential equation to fit the experimental data.

The asymptotic expression (the long-time behavior) for the fluorescence of ROH*(t) is given by[46]

$$I_L^{ROH^*} \exp(t/\tau) \cong \frac{\pi}{2} a^2 \exp(R_D/a) \frac{k_r}{k_d (\pi D)^{3/2}} t^{-3/2} \qquad (1)$$

In the above equation, τ is the excited-state lifetime, and R_D is the Debye radius given by

$$R_D = \frac{|z_1 z_2| e^2}{\epsilon k_B T} \qquad (2)$$

where z_1 and z_2 are the charges of the proton and anion, respectively, ϵ is the static dielectric constant of the solvent, and T is the absolute temperature. e is the electronic charge, and k_B is Boltzmann's constant. We estimate that the error in the determination of k_d is 5%. The error in the determination of k_d is due to (1) the signal-to-noise ratio of the experimental signal, which affects the fluorescence curve at longer times and (2) the interplay between k_d and k_r (see eq 1) at longer times. The uncertainty in the determination of k_r is estimated to be much larger, ~20%. The relatively large uncertainty in the values of k_r arises from the complex relation between the above-mentioned parameters that determine the ROH* fluorescence

tail and the large background due to the fluorescence of the impurity in the sample.

Modeling of the Proton Transfer to Water

General Considerations. The reaction of proton transfer to the solvent can be described schematically:

$$A^*H\cdot\cdot\cdot S_B \rightarrow A^{-}{}^*\cdot\cdot\cdot HS_B^+$$

The reactant is an intermolecular hydrogen-bonded complex between an excited photoacid, AH*, and a water molecule, S_B. S_B serves as a base, characterized by a hydrogen bond to the photoacid and also to other solvent molecules. In water, this specific water molecule, S_B, has three hydrogen bonds to three water molecules. To form the product $A^{-}{}^*\cdot\cdot\cdot HS_B^+$ in water, one hydrogen bond of S_B to a water molecule must be broken. Thus, a relatively long-range reorganization of the hydrogen bond network takes place upon proton transfer to the solvent. This complex rearrangement, to accommodate the product, is probably the reason for the slow solvent-generalized configuration motion that corresponds to a low-frequency component in the solvent dielectric spectrum. Its time constant is close to the slow component of the dielectric relaxation time. According to Kuznetsov and co-workers,[13−17] Borgis and Hynes,[18−20] Bernstein and co-workers,[47] and Syage,[48] a second important coordinate should be taken into account. This second coordinate is the distance between the two heavy atoms, O—H···O in our case. This distance is modulated by a low-frequency vibrational mode, Q.[18,47] The proton tunnels through the barrier from the reactant well to the product well via the assistance of the low-frequency Q mode whenever the solvent configuration equalizes the energies of the reactant and the product.

Borgis and Hynes[18−20] derived an expression for the proton-transfer rate constant, k. They wrote an expression for k in a transition-state theory form. k is expressed as the average one-way flux along the solvent coordinate, through the crossing point $S^{\ddagger}$ of the two free-energy surfaces, with the inclusion of a transmission coefficient, κ, giving the probability of a successful curve crossing:

$$k = \langle \dot{S}\,\Theta(\dot{S})\,\delta(S - S^{\neq})\,\kappa(\dot{S}, S^{\neq})\rangle_R \qquad (3)$$

where S is the generalized solvent coordinate, $\dot{S}$ is the solvent velocity, and $\Theta(\dot{S})$ is the step function. The brackets denote averaging over the classical solvent distribution normalized by the partition function of the solvent.

To find the appropriate nonadiabatic transmission coefficient,κ, for use in this equation, Borgis and Hynes[18] used the general Landau−Zener (LZ) transmission coefficient, κ, adapted for the present problem. The LZ factor, appropriate for a positive velocity approach to the crossing point, is

$$\kappa = [1 - {}^1/_2\exp(-\gamma)]^{-1}[1 - \exp(-\gamma)] \qquad (4)$$

where

$$\gamma = \frac{2\pi|V|^2}{\hbar\Delta F\dot{S}} = \frac{2\pi|V|^2}{\hbar k_S\dot{S}} \qquad (5)$$

is the adiabaticity parameter. The expression for the transmission coefficient κ includes multiple passage effects on the transition probability. V is the coupling matrix element between the reactant and the product, and ΔF is the slope difference of the diabatic potentials of mean force at the crossing point, $\Delta F = k_S$, where k_S is the parabolic potential-surface force constant. When $\gamma \ll 1$, one obtains the nonadiabatic-limit result

$$\kappa \cong 2\gamma \qquad (6)$$

leading to

$$k_{NA} = \frac{2\pi}{\hbar}|V|^2\left(\frac{\beta}{4\pi E_S}\right)^{1/2}\exp(-\beta\Delta G_{NA}^{\neq}) \qquad (7)$$

in which $\Delta G^{\ddagger}$ is the Marcus activation free energy

$$\Delta G_{NA}^{\neq} = \frac{1}{4E_S}(E_S + \Delta G)^2 \qquad (8)$$

The adiabaticity parameter, γ (see eq 5), depends on the potential surfaces curvature, ΔF, the coupling, $|V|^2$, and the velocity in the vicinity of crossing, $\dot{S}$. $|V|^2$ is independent of temperature. The solvent velocity, $\dot{S}$, however, depends strongly on temperature. In our previous papers,[7−10] we suggested that $\dot{S}$ is related to the slow components of the solvent relaxation. On the basis of the experimental data, we infer that $\dot{S} = b/\tau_D$, where τ_D is the solvent dielectric relaxation time and b is an empirical factor, dependent on the specific protic solvent, whose value is between 1 and 4.

In the adiabatic limit ($V \gg k_BT$, $\kappa \approx 1$), the adiabatic rate expression is

$$k_{AD} = (\omega_s/2\pi)\exp(-\beta\Delta G_{AD}^{\ddagger}) \qquad (9)$$

where ω_S is the solvent high frequency and $\Delta G_{AD}^{\ddagger} \cong \Delta G_{NA}^{\ddagger} - V$ is the free energy of activation.

Another physical limit is realized when $V \leq k_BT$ and the interaction with the environment is strong enough. In this solvent-controlled limit, the rate is inversely proportional to the solvent relaxation time (friction) and independent of the coupling V. Rips and Jortner[33] derived an expression for the resonant electron-transfer rate in the solvent-controlled limit.

$$k_{SC}^{ET} = \frac{1}{\tau_L}\left(\frac{E_S}{16\pi k_BT}\right)^{1/2}\exp(-\beta\Delta G_{NA}^{\neq}) \qquad (10)$$

For the nonresonance cases, the prefactor in the rate expression (eq 10) changes by only about 20%. τ_L is the longitudinal dielectric relaxation time $\tau_L = (\epsilon_\infty/\epsilon_S)\tau_D$, where ϵ_∞ and ϵ_S are the high-frequency and static dielectric constants, respectively.

The preexponent depends on the solvent's dynamical properties. At low temperatures, we found that the preexponential factor in the solvent-controlled limit is related to the slowest component of the dielectric relaxation time. We also found that the temperature dependence of the proton transfer can be explained as a continuous transition from the nonadiabatic limit at high temperature to the solvent-controlled limit at low temperature.

A number of attempts have been made to bridge these physical limits. Zusman[27] derived a rate expression that bridges the nonadiabatic limit and the solvent-controlled limit. Rips and Jortner have used a simple physical argument to obtain a rate expression that bridges all three limits.[31] They assumed that the crossover could be described in terms of a single dimensionless parameter, the ratio of the mean free path to the root-mean-square displacement of the reaction coordinate.

In our previous papers,[7−10] we used the mean-first-passage expression to bridge between the nonadiabatic limit and the solvent-controlled limit to obtain the rate expression

$$k_{PT}(T) = \frac{k_{NA}(T)\, k_{SC}(T)}{k_{NA}(T) + k_{SC}(T)} \tag{11}$$

where k_{PT} is the overall rate and k_{NA} and k_{SC} are given by eqs 7 and 10.

Numerical Calculation of the Proton-Transfer Rate. We use two crossing parabolic potential surfaces representing the free energy of the reactant and product along the solvent coordinate. For numerical calculation purposes, we focus our attention on the reactant single-well parabolic potential surface in the generalized solvent coordinate. The numerical calculation is based on the diffusive propagation of the solvent-generalized coordinate from the equilibrium position of the reactant well to the crossing point. We solve the Debye−Smoluchowski equation (DSE) for the specific problem. The probability density function, $p(S, t)$, to find a solvent configuration, S, along the generalized solvent coordinate at time t obeys the DSE[27,49,50]

$$\frac{\partial p(S,t)}{\partial t} = D\frac{\partial}{\partial S} e^{-\beta U(S)} \frac{\partial}{\partial S} e^{\beta U(S)}\, p(S, t) \tag{12}$$

where D is a diffusion constant and $U(S)$ is the potential surface.

In the numerical calculation, we used

$$U_r(S) = \frac{1}{2} k_S S^2$$

$$U_p(S) = \frac{1}{2} k_S (S - S_p)^2 \tag{13}$$

where $k_S = 2E_S$ and S is the generalized and normalized solvent coordinate. In this solvent coordinate, the reactant and product equilibrium positions are at $S_r = 0$ and $S_p = 1$, respectively. E_S is the solvent reorganization energy. For both 2N and 2N68DS, we used $E_S = 0.3$ eV. The calculation's initial condition is a thermal equilibrium of the probability density function, $p(S)$, of the solvent coordinate of the reactant and is given by a Gaussian distribution centered at the minimum of the reactant well.

$$p_{eq}(S) = \frac{1}{(2\pi\langle S^2\rangle)^{1/2}} \exp\left(-\frac{S^2}{2\langle S^2\rangle}\right) \tag{14}$$

where $\langle S^2\rangle$ is the mean square displacement with a Gaussian width of $U(\langle S^2\rangle) = \sqrt{2E_S k_B T}$.

The diffusion constant, D, is related to the dielectric relaxation time, τ_D, and the widths of the Gaussian initial distribution,[49] $D = \langle S^2\rangle/2\tau_S$, $\tau_S = \tau_D/b$, where b is an empirical factor. For $E_S = 0.3$ eV, $\langle S^2\rangle \cong 0.16$ at room temperature.

The activation energy, $\Delta G^{\ddagger}$, to cross between the reactant well and the product well is determined from the experimental activation energy measured at high temperatures (the nonadiabatic limit). For 2N68DS, we used $\Delta G^{\ddagger} \approx 2.5$ kJ/mol. The position of the activation barrier is determined by $\Delta G^{\ddagger} = U(S^{\ddagger})$ and $S^{\ddagger} = 0.21$. For 2N, we used $\Delta G^{\ddagger} \approx 12$ kJ/mol and calculated $S^{\ddagger} = 0.37$.

The next step in the calculation is based upon solving the DSE of a single parabolic potential surface with the relevant initial and boundary conditions. To solve it, we used a modification of a user-friendly graphic program, SSDP (Ver. 2.61), of Krissinel and Agmon.[51] The modification is based on using the Landau−Zener transmission coefficient, κ (eq 4), in the sink term at the crossing point between the reactant well and the product well. The boundary condition at the crossing point is given by

$$\left.\frac{\partial p}{\partial S}\right|_{S=S^{\neq}} = -k_0 \kappa \dot{S} p(S^{\neq}, t) \tag{15}$$

The boundary condition (eq 15) we chose has similar components to the expression for the rate constant, expressed in a transition-state theory form (eq 3). The average solvent velocity, $\dot{S}$, is proportional to $1/\tau_D$, κ appears in both expressions, k_0 is a numerical factor that is independent of temperature and is determined by fitting the numerical solution to the experimental proton-transfer rate constant at high temperatures.

Finally, the proton-transfer rate constant is obtained from the slope of the plot of $\ln(p)$ versus time.

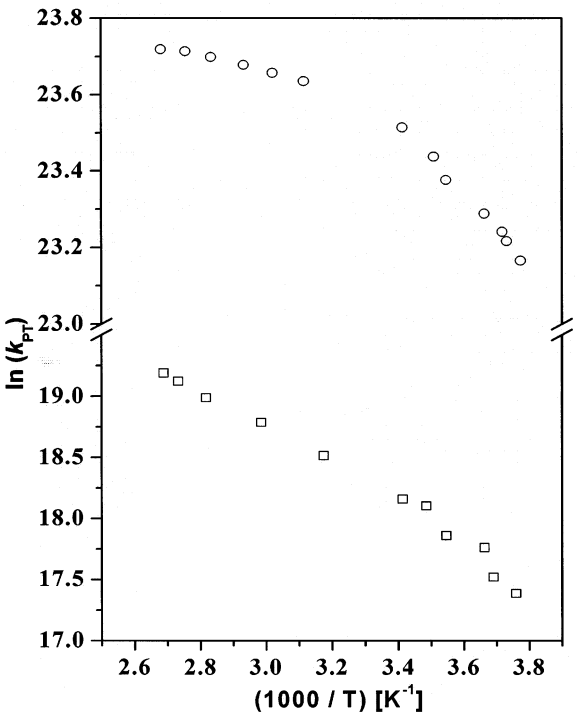

Figure 1. Proton-transfer rate constant as a function of $1/T$ for 2N68DS (○) and 2N (□).

Results

2-Naphthol-6,8-disulfonate. Figure 1 shows the proton-transfer rate constant for both 2N68DS (circles) and 2N (squares) as a function of $1/T$. The temperature dependence of the proton-transfer rate constant, k_{PT}, of 2N68DS is quite unusual for chemical reactions. In general, chemical reactions obey a constant exponential (Arrhenius) decrease of the reaction rate constant as a function of $1/T$ over a large temperature range. As described previously, the value of k_d is nearly insensitive to the solvent temperature at $T > 300$ K, whereas below 300 K, k_d decreases with the decrease in the sample temperature with a temperature-dependent activation energy.

Figure 2 shows the activation energy of the proton-transfer rate constant of 2N68DS (circles) in water as a function of T^{-1}. In the high-temperature range, $T > 300$ K, the activation energy is almost constant, with an average value of about 2.5 kJ/mol, whereas in the low-temperature region, it changes from 4 kJ/mol at about 300 K up to 10 kJ/mol at 265 K.

Figure 3a shows the experimental results along with the calculated results using the DSE for the proton-transfer reaction

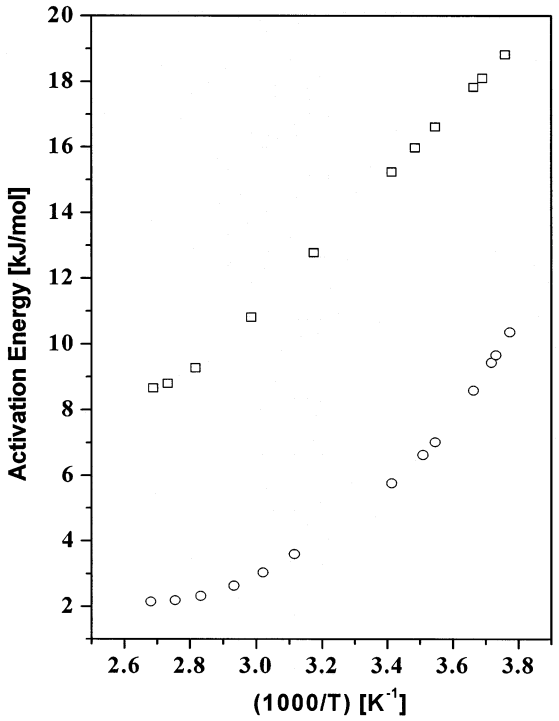

Figure 2. Activation energy of the proton transfer rate of 2N68DS (○) and 2N (□) as a function of $1/T$.

from 2N68DS to aqueous solution as a function of T^{-1}. Full circles represent the computed rates; open squares represent the experimental rates. The solid line is from a calculation based on the mean-first-passage expression (eq 11). The relevant parameters for the calculation using the diffusion model are given in Table 1.

The rate constant calculated using the interpolation equation (eq 11) (the solid line in Figure 3a) also gives a good fit to the experimental data. For 2N68DS, we evaluate from the high-temperature data $V \approx 2$ cm^{-1}. The free adjustable parameters in the calculation are γ', b, and k_0:

$$\gamma = \gamma' \tau_D(T) \tag{16}$$

We find that $\gamma' = 1.6 \times 10^{10}$ s^{-1} from the best fit to the experimental data for the rate of proton transfer of 2N68DS to water and that $b = 2.5$ and $k_0 = 350$ Å/ns.

2-Naphthol. Figure 1 shows on a semilog scale an Arrhenius plot of the proton-transfer rate constant for 2N (circles). The proton-transfer rate constant from 2N (p$K^* = 2.7$) to water at room temperature is relatively small ($\sim 10^8$ s^{-1}), and it exhibits a relatively strong temperature dependence even at high temperatures, $T > 300$ K. This behavior is in contrast to our findings for stronger photoacids such as 2N68DS ($k_{PT} \approx 2 \times 10^{10}$ s^{-1}) with p$K^* \approx 0.4$ and a previously studied photoacid 8-hydroxy-1,3,6-trisulfonate (HPTS) with p$K^* \approx 1$.[7]

The activation energy of 2N is not constant (see Figure 2, squares). At high temperatures, $T > 320$ K, we find that $\Delta G^{\ddagger} = 10$ kJ/mol, whereas at supercooled temperatures, $\Delta G^{\ddagger} \approx 18$ kJ/mol. The experimental data of ln k_{PT} versus $1/T$ can be fitted with our model. Figure 3b shows the plot of the proton-transfer rate constant, k_{PT}, as a function of T^{-1}; the experimental data (squares), the computed values (circles), and the solid line are from the computation based on the interpolation equation (eq 11). For the adjustable parameters, we find $\gamma' = 6 \times 10^9$ s^{-1}, $b = 1.2$, and $k_0 = 320$ Å/ns. Both $|V|^2$ and the activation energy

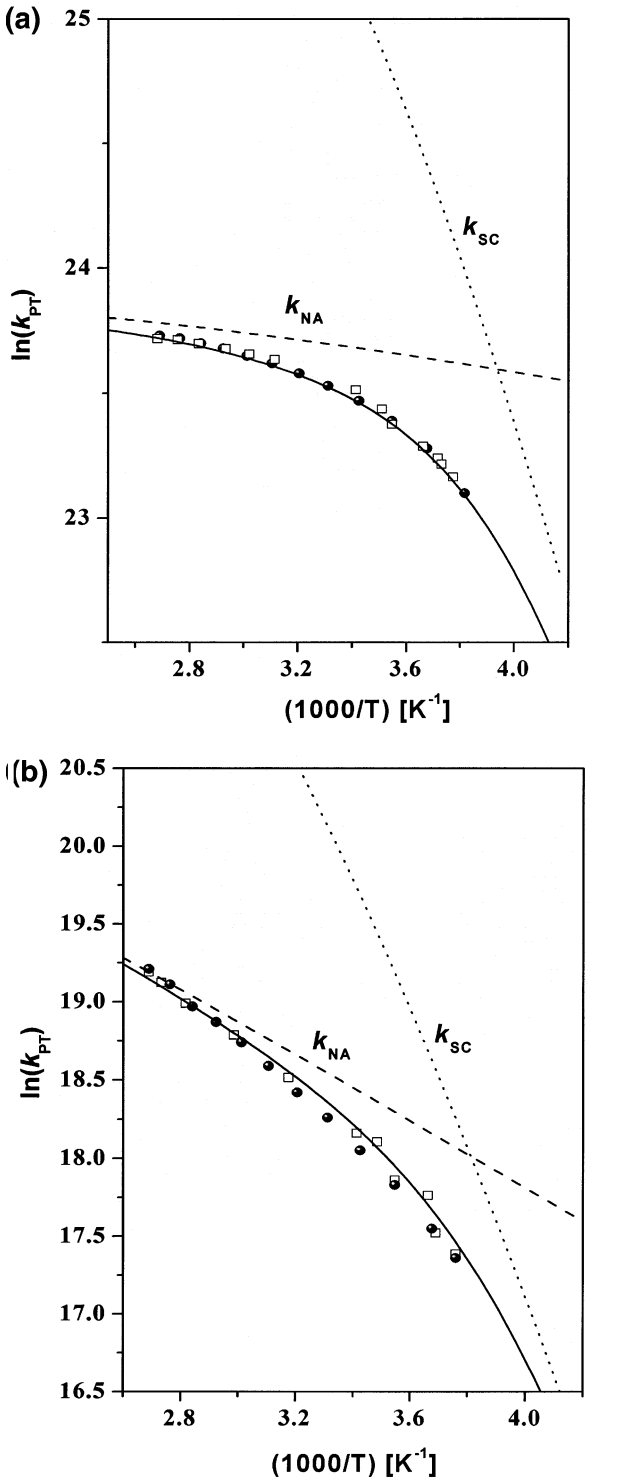

Figure 3. Semilogarithmic plot of the proton-transfer rate constant from photoacid to water versus T^{-1} for (a) 2N68DS and (b) 2N. Experimental data (□), calculations according to our diffusive model and LZ boundary condition (●), and the interpolation equation using eq 11 (—).

were determined from the high-temperature data, $V \approx 1$ cm^{-1} and $\Delta G^{\ddagger} \approx 11$ kJ/mol.

Discussion

In this paper, we measure and calculate the proton-transfer rate constant from two photoacids—a weak photoacid, 2-naphthol with p$K^* = 2.7$ and a relatively strong one, 2-naphthol-6,8-disulfonate with p$K^* \approx 0.4$—to water as a function of

TABLE 1: Relevant Parameters for Model Calculations of $^{a}E_s = 0.3$ eV, $^{b,c}S_r = 0$, and $S_p = 1$ Å

	^{d} pK^*	$^{e}\Delta G^{\ddagger}$ [kJ/mol]	$^{f}\Delta G^{\ddagger}$ [kJ/mol]	$^{g}S^{\ddagger}$	$^{h}k_{NA}^{PT}$ [s^{-1}]	$^{b,i}k_0$ [Å/ns]	$^{j}\gamma'$	$^{k}\gamma''$	^{l}V [cm^{-1}]	^{m}b
2N	2.7	17	11.5	0.39	1.9×10^8	320	6×10^9	6.6×10^9	0.98	1.2
2N68DS	0.4	9	2.5	0.21	1.9×10^{10}	350	1.6×10^{10}	1.8×10^{10}	2.3	2.5

[a] Solvent reorganization energy. [b] For calculations with the SSDP program,[51] we used the solvent coordinate with a length dimension of angstroms. [c] We placed the minima of the reactant and product potential surfaces at 0 and 1 Å, respectively. [d] Excited-state equilibrium constant. [e] Activation energy as calculated from eq 8. [f] Activation energy obtained by the best fit to the experimental data. [g] Crossing-point position between the two diabatic potential surfaces. [h] Experimental values of the PT rate constant at 373 K. [i] k_0 is a numerical factor that is independent of temperature and is determined by fitting the numerical solution to the experimental proton-transfer rate constant at high temperatures. [j] γ' is a free adjustable parameter (see eq 16). [k] γ'' is the calculated value of γ' according to $\gamma'' = \frac{2\pi}{\hbar}|V|^2 \frac{1}{\Delta F}\frac{1}{b}$. [l] Evaluated from the experimental high-temperature rate constant. [m] Empirical factor used in the determination of the proton transfer rate.

temperature and correlate the results with the corresponding values of the dielectric relaxation time, τ_D. In our previous studies,[8−10] we found that the temperature dependence of the proton-transfer rate constant from a superphotoacid, 5,8-dicyano-2-naphthol (DCN2) (with p$K_a^* = -4.5$ in water), to alcohols exhibits non-Arrhenius behavior. We found that, at low temperatures, the proton-transfer rate constant follows the inverse of τ_D (i.e., $k_{PT} = b/\tau_D$), where b is an empirical factor and its value for methanol is ∼2. The proton-transfer rate constant of the strong photoacid, 2N68DS, exhibits a similar temperature dependence. Unlike the temperature dependence of the proton-transfer rate constant of 2N68DS from the weaker photoacid 2N, the proton-transfer rate constant also exhibits great temperature dependence at high water temperature. In the current paper, we used a similar approach to explain and calculate the temperature dependence of both 2N68DS and 2N.

Conventional Landau−Zener (LZ) theory[11,12] provides an accurate description of the curve-crossing process if the motion in the vicinity of the crossing point is nearly uniform (ballistic).[25,26] Rips and Pollak[34] showed that variational transition-state theory (VTST) allows for the identification of a collective coordinate along which the dynamics in the curve-crossing region is maximally separated from the remaining solvent-induced dynamics (quasiballistic). The rate of transition from the reactant to the product wells can then be calculated by conventional LZ theory.

In a recent paper,[52] we used the same model as used in this paper to fit the experimental temperature dependence of the proton transfer from DCN2 to methanol and glycerol. The model is based on a diffusive propagation of the solvent configuration along a generalized solvent coordinate from the reactant potential surface toward the crossing point with the product potential surface. The proton transfer occurs at the crossing point, and the rate is calculated by a sink term placed at the crossing point. The sink term includes the solvent velocity and the Landau−Zener transmission coefficient. Both the diffusion constant and the Landau−Zener transmission coefficient depend on the dielectric relaxation of the solvent. Our model calculations show that, for sufficiently strong photoacids, at high temperatures (the nonadiabatic limit), the generalized water configuration motion is fast, the activation energy is sufficiently low, and the proton tunneling rate is the rate-determining step. The LZ transmission coefficient is small and hence limits the rate of population transfer to the product (in our model, successful crossing of population to the product diabatic potential surface). From the rate constant at high temperatures (the nonadiabatic limit, eq 7), we determine the preexponential factor and the activation energy of the process.

The preexponential factor is mainly determined by the value of the coupling matrix element. The transmission coefficient from the reactant well to the product well at the crossing point (at the top of the barrier) is given by the Landau−Zener transmission coefficient (eq 4). The adiabaticity parameter, γ (eq 7), is determined by three parameters: $|V|^2$, ΔF, and $\dot{S}$. $|V|^2$ can be evaluated from the experimental high-temperature rate constant. We find that the preexponential factor is 1.1×10^{11} s^{-1} and 8×10^9 s^{-1} for 2N68DS and 2N, respectively. From the preexponential expression, we evaluate V to be ∼2 and 1 cm^{-1} for 2N68DS and 2N, respectively. $\Delta F = k_S$, where k_S is the mean force constant, which is related to the solvent reorganization energy, $k_S = 2E_S$. The medium reorganization energy E_s can be calculated for spherical ions.[49] The charge distributions of naphthol derivatives and naphtholate derivatives are complex, and it is a difficult task to estimate E_s. For polar liquids, it is customary to use E_s values in the range of 0.1−0.3 eV.[18,53] For both compounds, we used the same reorganization energy, $E_S = 0.3$ eV. To evaluate the adiabaticity parameter $\gamma = \gamma''\tau_D$ quantitatively, we calculate the value of

$$\gamma'' = \frac{2\pi}{\hbar}|V^2|\frac{1}{\Delta F}\frac{1}{b} \cong 1.8 \times 10^{10}\ \mathrm{s}^{-1}$$

for 2N68DS. For 2N, we find $\gamma'' \approx 7 \times 10^9$ s^{-1}.

In our previous work,[52] we found the proton transfer rate from the superphotoacid DCN2 to methanol or glycerol, and at a low enough temperature (the solvent-controlled limit), the diffusive propagation of the solvent configuration toward the crossing region is slow compared to the tunneling rate. The LZ transmission coefficient is close to 1 since the average solvent velocity, $\dot{S}$, is slow (eq 5) and the rate-determining step is the transport motion of the probability density function of the solvent configuration itself, which also appears in the sink term (eq 15). The activation energy of the process, $\Delta G^{\ddagger}$, remains small, but the diffusion constant, which is related to the average velocity of the solvent configuration, exhibits a large temperature dependence. In the solvent-controlled-limit rate expression (eq 10), the preexponential factor of the electron-transfer rate constant is determined by τ_L. For the analysis and the data fit, we use the average generalized solvent configuration velocity at the crossing point, $\dot{S} = b/\tau_D$, where b is an empirical factor.

From previous studies on alcohols[7−10,52] and also in this study, we find that the solvent characteristic time for proton transfer, $\tau_S = \tau_D/b$, is in the range $\tau_D > \tau_S > \tau_L$, where $\tau_L = (\epsilon_\infty/\epsilon_S)\tau_D$ is the longitudinal dielectric relaxation time. For methanol, we found the value of the empirical factor $b \approx 2$, and for 2N68DS in water, we found a slightly larger value, $b = 2.5$, whereas for 2N, this factor was significantly smaller, $b = 1.2$. The values of τ_L for water can be estimated from the values of the low- and high-frequency dielectric constants of water, ϵ_S and ϵ_∞, which are relevant for the proton-transfer process. The static dielectric constant of water is $\epsilon_S^{water} = 78$ at 298 K. The description of the dielectric relaxation literature results for water requires a superposition of two Debye processes.[54−56] The high-frequency dielectric constant of the slower process is about

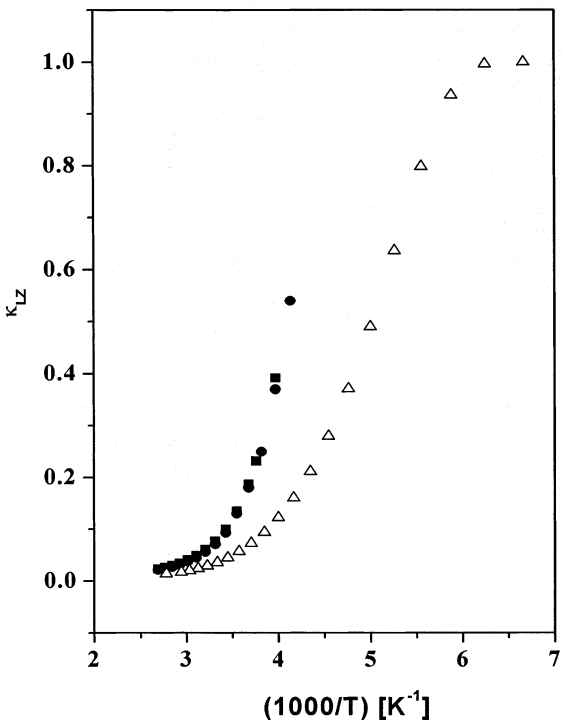

Figure 4. Calculated Landau−Zener transmission coefficient, κ_{LZ}, as a function of T^{-1} for the proton-transfer reaction from 2N68DS (●) and 2N (■) to water. κ_{LZ} for DCN2 to methanol is also shown (△); results were taken from ref 52.

$\epsilon = 6.5$, and the dielectric relaxation times range from ∼6 ps at 310 K to 18 ps at 273 K. The faster process that contributes the second Debye relaxation time has a duration of about 1 ps; its high-frequency dielectric constant is about 4.5 and is almost temperature-independent. The ratio for the slow process, $\epsilon_S/\epsilon_\infty$, is 12, whereas we find from the fitting of the proton-transfer process from 2N and 2N68DS much smaller values, $b = 1.2$ and 2.5, respectively. $\tau_L^{293K} = 0.8$ ps, and τ_S for 2N and 2N68DS in our calculations is about 8 and 4 ps, respectively.

In the calculation of the proton-transfer rate constant, on the basis of the Landau−Zener curve-crossing formulation, we find that for both compounds, 2N and 2N68DS, at 373 K, the boiling point of water, the reaction is in the nonadiabatic regime, $\kappa_{LZ} = 0.02$. At room temperature, κ_{LZ} increases only slightly and is about 0.07, which means that the reaction is still in the nonadiabatic regime. The rate-limiting step is the proton motion, whereas the dynamics of the solvent configuration is fast and does not limit the rate of proton transfer. At 252 K, the adiabaticity parameter increases significantly, $\gamma = 0.27$ and $\kappa_{LZ} \approx 0.3$. Thus, for supercooled water, $T = 252$ K, the rate constant is determined by the dynamics of both coordinates, the solvent configuration, and the proton tunneling. As discussed above in the case of proton transfer from DCN2 to alcohols, we were able to observe a continuous transition from the nonadiabatic regime, $\kappa_{LZ} < 0.1$, to the solvent-controlled limit, $\kappa_{LZ} > 0.9$, by continuously changing the temperature from high to low. In Figure 4, we plot the Landau−Zener transmission coefficient as a function of $1/T$ for the photoacids studied, and for comparison, we also display our previous results[52] of κ_{LZ} for the proton-transfer reaction from DCN2 to methanol (triangles). As seen for DCN2, κ_{LZ} reaches a value of 1, the solvent-controlled limit, at about 170 K, close to the freezing point of methanol. The midtransition point of the Landau−Zener transmission coefficient, $\kappa_{LZ} = 0.5$, for methanol occurred at 200 K. In the current case of proton transfer from both 2N and 2N68DS to water, even under the supercooled condition of 250 K, $\kappa_{LZ} = 0.3$, and hence the reaction-rate constant is mostly determined by the proton tunneling rate, and the solvent dynamics limit the reaction rate to a lesser extent.

From our calculation, it arises that at high temperatures down to about room temperature, ∼300 K, the proton-transfer rate constant is nearly independent of the generalized solvent configuration motion since it is faster than the tunneling rate. Only at lower temperatures, solvent motion partially controls the proton-transfer process, and the value of the rate constant is influenced thereby. The experimental activation energy of proton transfer processes from 2N68DS increases by a factor of approximately 5 since the relevant water motion that governs the proton transfer process strongly depends on the temperature of supercooled water.

Acknowledgment. We thank Professor I. Rips and Professor N. Agmon for their helpful discussions. This work was supported by grants from the US−Israel Binational Science Foundation and the James−Franck German−Israel Program in Laser-Matter Interaction.

References and Notes

(1) Ireland, J. F.; Wyatt, P. A. H. *Adv. Phys. Org. Chem.* **1976**, *12*, 131.
(2) Huppert, D.; Gutman, M.; Kaufmann, K. J. *Adv. Chem. Phys.* **1981**, *47*, 681. Koswer, E.; Huppert, D. *Annu. Rev. Phys. Chem.* **1986**, *37*, 122.
(3) Lee, J.; Robinson, G. W.; Webb, S. P.; Philips, L. A.; Clark, J. H. *J. Am. Chem. Soc.* **1986**, *108*, 6538.
(4) Gutman, M.; Nachliel, E. *Biochim. Biophys. Acta* **1990**, *391*, 1015.
(5) Förster, Th. *Z. Natuwiss.* **1949**, *36*, 186.
(6) Weller, A. *Prog. React. Kinet.* **1961**, *1*, 189.
(7) Poles, E.; Cohen, B.; Huppert, D. *Isr. J. Chem.* **1999**, *39*, 347.
(8) Cohen, B.; Huppert, D. *J. Phys. Chem. A* **2000**, *104*, 2663.
(9) Cohen, B.; Huppert, D. *J. Phys. Chem. A* **2001**, *105*, 2980.
(10) Cohen, B.; Huppert, D. *J. Phys. Chem. A* **2002,** *106*, 1946.
(11) Landau, L. D. *Phys. Z. Sowjetunion* **1932**, *1*, 88. Landau, L. D. *Phys. Z. Sowjetunion* **1932**, *2*, 46.
(12) Zener, C. *Proc. R. Soc. London, Ser. A* **1932**, *137*, 696
(13) German, E. D.; Dogonadze, R. R.; Kuznetsov, A. M.; Levich, V. G.; Kharkats, Yu. I. *Elektrokhimiya* **1970**, *6*, 350.
(14) German, E. D.; Kuznetsov, A. M.; Dogonadze, R. R. J. *Chem. Soc., Faraday Trans. 2* **1980**, *76*, 1128.
(15) German, E. D.; Kuznetsov, A. M. *J. Chem. Soc., Faraday Trans. 1* **1981**, *77*, 397.
(16) German, E. D.; Kuznetsov, A. M. *J. Chem. Soc., Faraday Trans. 2* **1981**, *77*, 2203.
(17) Kuznetsov, A. M. *Charge Transfer in Physics, Chemistry and Biology: Physical Mechanisms of Elementary Processes and an Introduction to the Theory;* Gordon and Breach: Amsterdam, 1995.
(18) Borgis, D.; Hynes, J. T. *J. Phys. Chem.* **1996**, *100*, 1118.
(19) Borgis, D. C.; Lee, S.; Hynes, J. T. *Chem. Phys. Lett.* **1989**, *162*, 19.
(20) Borgis, D.; Hynes, J. T. *J. Chem. Phys.* **1991**, *94*, 3619.
(21) Cukier, R. I.; Morillo, M. *J. Chem. Phys.* **1989**, *91*, 857.
(22) Morillo, M.; Cukier, R. I. *J. Chem. Phys.* **1990**, *92*, 4833.
(23) Li, D.; Voth, G. A. *J. Phys. Chem.* **1991**, *95*, 10425.
(24) Lobaugh, J.; Voth, G. A. *J. Chem. Phys.* **1994**, *100*, 3039.
(25) Landau, L. D.; Lifshitz, E. M. *Quantum Mechanics: Nonrelativistic Theory*; Pergamon Press: New York, 1977; Section 90.
(26) Nikitin, E. E.; Umanskii, S. Y. *Theory of Slow Atomic Collisions;* Springer: Berlin, 1984; Chapter 8.
(27) Zusman, L. D. *Chem. Phys.* **1980**, *49*, 295.
(28) Yakobson, B. I.; Burshtein, A. I. *Chem. Phys.* **1980**, *49*, 385.
(29) Calef, D. F.; Wolynes, P. G. *J. Phys. Chem.* **1983**, *87*, 3387.
(30) Frauenfelder, H.; Wolynes, P. G. *Science (Washington, D.C.)* **1985**, *229*, 337.
(31) Rips, I.; Jortner, J. *J. Chem. Phys.* **1987**, *87*, 2090.
(32) Straub, J. E.; Berne, B. J. *J. Chem. Phys.* **1987**, *87*, 6111.
(33) Rips, I.; Jortner, J. In *Perspectives in Photosynthesis*; Jortner, J., Pullman, B., Eds.; Kluwer: Dordrecht, The Netherlands, 1990; p 293.
(34) Rips, I.; Pollak, E. *J. Chem. Phys.* **1995**, *103*, 7912.
(35) Rips, I. *J. Chem. Phys.* **1996**, *24*, 9795.
(36) Pines, E.; Huppert, D.; Agmon, N. *J. Chem. Phys.* **1988**, *88*, 5620.
(37) Agmon, N.; Pines, E.; Huppert, D. *J. Chem. Phys.* **1988**, *88*, 5631.
(38) Debye, P. *Trans. Electrochem. Soc.* **1942**, *82*, 265.

(39) Robinson, R. A.; Stokes, R. H. *Electrolyte Solutions: The Measurement and Interpretation of Conductance, Chemical Potential and Diffusion in Solutions of Simple Electrolytes*, 2nd ed.; Butterworths: London, 1959.
(40) Erdey-Gruz, T.; Lengyel, S. In *Modern Aspects of Electrochemistry*; Bockris, J. O'M., Conway, B. E., Eds.; Plenum Publishing: New York, 1964; Vol. 12, pp 1−40.
(41) Hallett, J. *Proc. Phys. Soc., London* **1963**, *82*, 1046.
(42) Eicher, L. D.; Zwolinski, B. J. *J. Phys. Chem.* **1971**, *75*, 2016.
(43) Bertolini, D.; Cassettari, M.; Salvetti, G. *J. Chem. Phys.* **1982**, *76*, 3285.
(44) Kaatze, U. *J. Chem. Eng. Data* **1989**, *34*, 371.
(45) Nabokov, O. A.; Lubimov, Y. A. *Mol. Phys.* **1988**, *65*, 1473.
(46) Agmon, N.; Goldberg, S. Y.; Huppert, D. *J. Mol. Liq.* **1995**, *64*, 161.
(47) Hineman M. F.; Brucker G. A;, Kelley D. F.; Bernstein, E. R. *J. Chem. Phys.* **1992**, *97*, 3341.
(48) Syage, J. A. *J. Phys. Chem.* **1995**, *99*, 5772.
(49) Sumi, H.; Marcus, R. A. *J. Chem. Phys.* **1986**, *84*, 4272. Sumi, H.; Marcus, R. A. *J. Chem. Phys.* **1986**, *84*, 4894.
(50) Agmon, N.; Hopfield, J. J. *J. Chem. Phys.* **1983**, *78*, 6947.
(51) Krissinel, E. B.; Agmon, N. *J. Comput. Chem.* **1996**, *17*, 1085.
(52) Cohen, B.; Segal, J.; Huppert, D. *J. Phys. Chem. A* **2002**, *106*, 7462.
(53) Peters, K. S.; Cashin A. *J. Phys. Chem. A* **2000**, *104*, 4833.
(54) Barthel, J.; Bachhuber, K.; Buchner, R.; Hetzenauer, H. *Chem. Phys. Lett*. **1990**, *165*, 369.
(55) Barthel, J.; Bachhuber, K.; Buchner, R.; Gill, J. B.; Kleebauer, M. *Chem. Phys. Lett*. **1990**, *167*, 62.
(56) Buchner, R.; Barthel, J. *J. Mol. Liq.* **1995**, *63*, 55.